HAL
open science

Diffusion of interstitial species (H and O atoms) in fcc systems (Al, Cu, Co, Ni and Pd): Contribution of first and second order transition states

Damien Connétable, Matthieu David

To cite this version:

Damien Connétable, Matthieu David. Diffusion of interstitial species (H and O atoms) in fcc systems (Al, Cu, Co, Ni and Pd): Contribution of first and second order transition states. Journal of Alloys and Compounds, 2019, 772, pp.280-287. 10.1016/j.jallcom.2018.09.042 . hal-01996439

HAL Id: hal-01996439

https://hal.science/hal-01996439v1

Submitted on 28 Jan 2019

HAL is a multi-disciplinary open access archive for the deposit and dissemination of scientific research documents, whether they are published or not. The documents may come from teaching and research institutions in France or abroad, or from public or private research centers.

L'archive ouverte pluridisciplinaire **HAL**, est destinée au dépôt et à la diffusion de documents scientifiques de niveau recherche, publiés ou non, émanant des établissements d'enseignement et de recherche français ou étrangers, des laboratoires publics ou privés.

Open Archive Toulouse Archive Ouverte (OATAO)

OATAO is an open access repository that collects the work of Toulouse researchers and makes it freely available over the web where possible

This is an author's version published in: http://oatao.univ-toulouse.fr/21427

Official URL: https://doi.org/10.1016/j.jallcom.2018.09.042

To cite this version:

Connétable, Damien and David, Matthieu *Diffusion of interstitial species (H and O atoms) in fcc systems (Al, Cu, Co, Ni and Pd): Contribution of first and second order transition states.* (2019) Journal of Alloys and Compounds, 772. 280-287. ISSN 0925-8388

Any correspondence concerning this service should be sent to the repository administrator: tech-oatao@listes-diff.inp-toulouse.fr

Diffusion of interstitial species (H and O atoms) in fcc systems (Al, Cu, Co, Ni and Pd): Contribution of first and second order transition states

Damien Connétable [a, b, *], Matthieu David [a, b]

[a] CIRIMAT, CNRS, Toulouse, France
[b] CIRIMAT-ENSIACET, 4 Allée Émile Monso, BP 44362, F-31030 Toulouse Cedex 4, France

ARTICLE INFO

Keywords:
Diffusion
Hydrogen and oxygen
Metallic systems
DFT calculations

ABSTRACT

We present a discussion on the influence of high-order transition states on interstitial diffusion in fcc systems using first-principles calculations. In earlier works, only first-order transition states (1TS) were used to compute the diffusivity at the atomic-scale: the direct diffusion between tetrahedral (*t*) and octahedral (*o*) sites has been proposed to describe atomic-scale diffusion mechanisms. However, we show here that if this direct diffusion makes it possible to reproduce displacements remarkably well, neglecting higher-order transition states induces an underestimation of the diffusion coefficient at high temperature. We hereinafter revisit the diffusion coefficient of interstitial species in different fcc-systems. The effect of these configurations on atom diffusion in Al, Co, Cu, Ni and Pd, whose only stable sites are the tetrahedral and octahedral positions (H and O atoms) is thus discussed here. We show that if the correction is low, taking into account higher-transition states can modify the diffusivity values at high temperature.

1. Introduction

The diffusion mechanisms of atoms in interstitial position are now commonly studied in solid-state physics, as the growing amount of work [1–5] on the matter indicates. If the possibility of forming clusters with vacancies, the interactions with defects or the interfaces of the network are ignored, the atomic process of diffusion of interstitial species is controlled, in first-order approximation, by the energy landscape defined by the network. Atoms then diffuse from one stable site to another. However, these stable sites are not necessarily equivalent from a geometrical standpoint. In the case of fcc systems, where tetrahedral and octahedral sites are often the most stable sites, direct diffusion between *t* and *o* sites is (almost) systematically used to describe and predict atomic-scale diffusion. Wimmer et al. [2] proposed an explicit diffusion coefficient formula taking into account these two stable sites with a single jump, using the jump rates from *o* to *t* sites, "Γ_{o-t}". In the literature, various authors have considered that direct transitions between first-nearest neighboring octahedral or tetrahedral sites should be ignored in the calculation of the diffusion coefficient, due to a high migration energy. As shown by David et al. [4], this transition state is always set in the *M* site, which is located exactly between two nearest octahedral sites, between two nearest tetrahedral sites and between two fcc sites (see Fig. 1). From a geometrical standpoint, when an interstitial atom is located an *M* site, it can move directly into four different stable sites.

By studying the vibrational properties of interstitial atoms in different positions, results have shown that, in Al [4], these calculated transition states necessarily present two imaginary branches associated with the moving atom. These mechanisms should therefore be included in the transition theory in addition to the direct *o*-*t* path. However, most solid-state physics works do not discuss the possibility of interstitial diffusion through these configurations. Most expressions of diffusion equations generally do not include this option.

In this paper, we look back at the often overlooked question of taking these paths into account. We compare the diffusion mechanisms between *t* and *o* sites found in two proven cases (H and O atoms) by taking into account the first-order transition state (direct diffusion path between o and t) but also second-order transition states (2TS) by taking into account *M* site or not. The case of H atoms in Al, Cu, Co, Ni and Pd, and O atom in Ni, Cu, Co and Pd are suitable cases to illustrate our point. This study also entails the opportunity of a detailed discussion on H and O diffusion

* Corresponding author. CIRIMAT, CNRS, Toulouse, France.
E-mail address: damien.connetable@ensiacet.fr (D. Connétable).

https://doi.org/10.1016/j.jallcom.2018.09.042

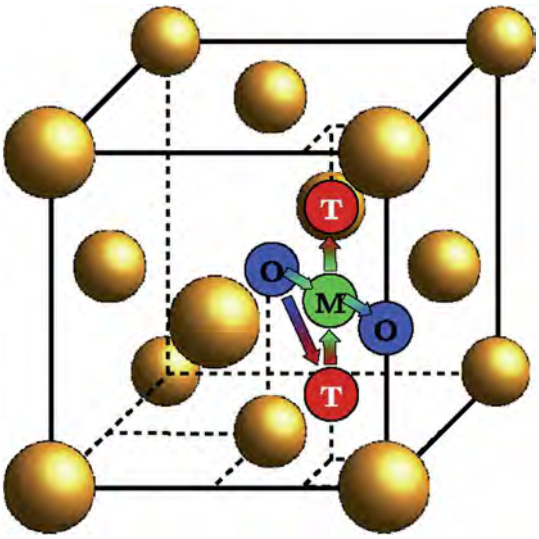

Fig. 1. Position of main specific sites in fcc structures: octahedral (o), tetrahedral (t), and M sites. The different diffusion paths are also depicted.

mechanisms in various fcc metals, which, in some cases, has never been carried out. Our study was conducted by examining the mechanisms of diffusion at the atomic scale using first-principles calculations, and using the Eyring theory, with explicit equation of diffusion coefficients. We hereby study the effect of including 2TS in the atomistic process of diffusion.

2. Methodology

Calculations were performed using the Vienna *ab initio* simulation package (VASP) [6]. Self-consistent Kohn-Sham equations were solved using the projector augmented wave (PAW) pseudo-potentials [7]. We used the Perdew-Burke-Ernzerhof [8] exchange and correlation functional. The plane-wave energy cut-off was set to 600 eV and Γ-centered Monkhorst-Pack meshes [9] were used to sample the first Brillouin zone (equivalent to $20 \times 20 \times 20$ for cubic cells, i.e. with 4 atoms). A super-cell approach was used with full periodic boundary conditions to describe systems with and without point defect: $3 \times 3 \times 3$ super-cells to compute formation energies and $2 \times 2 \times 2$ super-cells to compute inter-atomic force constants (IFC) and migration energies. Atomic positions and lattice parameters (shapes and volumes) were fully relaxed. In the case of Ni and Co atoms, simulations were performed with magnetism, which was not the case for Al, Cu and Pd.

Vibrational properties and inter-atomic force constants (IFCs) were obtained as finite differences of forces with respect to atomic displacements fields. The *phonopy* package [10] was used to generate finite displacements according to the symmetry of each structure. The *phonopy* package was then used to analyze, plot vibrational properties (phonon band structures and density-of-states, not shown here) and compute vibrational partition functions. In all cases discussed here, the full inter-atomic vibrational forces of the super-cells were computed, for stable and transition states.

We used the Eyring transition state theory [11] to examine diffusion coefficients. According to this theory, all transition states should be included in atomistic mechanisms. It is therefore also important they be taken into account, especially first- and second-order transition states. The characteristic quantity, commonly used to quantify the probability of leaving a site, is the jump rate, Γ, computed by using the following equation:

Table 1
Formation energies (E_f, in eV), zero-point energy (ZPE, in meV), formation enthalpies (H_f, in eV), and migration energies E_m from o (resp. t) to t (resp. o) (in eV). Frequencies of H_2 and O_2 are equal to 583.6 and 193.8 meV, respectively. Some data are extracted from Refs. [4,14]. The asterisk (*) indicates activation energies obtained with NEB calculations on larger super-cells ($3 \times 3 \times 3$).

	E_f	ZPE	H_f	E_m	E_f	ZPE	H_f	E_m
	Al H							
o	0.823	−68	0.755	0.06				
t	**0.717**	13	0.730	0.17				
M	1.042	unstable						
	Cu H				Cu O			
o	**0.430**	−24	0.406	0.30/0.29*	**0.086**	−21	0.065	0.40
t	0.631	57	0.688	0.15/0.09*	0.427	−4	0.423	0.20
M	0.969	unstable			0.781	unstable		
	Co H				Co O			
o	**0.128**	16	0.144	0.46	**−0.131**	20	−0.111	0.94
t	0.418	91	0.509	0.17	0.594	31	0.563	0.24
M	0.970	unstable			1.222	unstable		
	Ni H				Ni O			
o	**0.063**	−81	−0.018	0.37	**0.487**	−23	0.465	0.75
t	0.323	0	0.323	0.11	0.650	−4	0.645	0.53
M	0.814	unstable			1.265	unstable		
	Pd H				Pd O			
o	**−0.119**	−85	−0.208	0.15	1.077	−41	1.036	0.27
t	−0.075	36	−0.058	0.11	**0.651**	15	0.666	0.72
M	0.320	unstable			1.734	unstable		

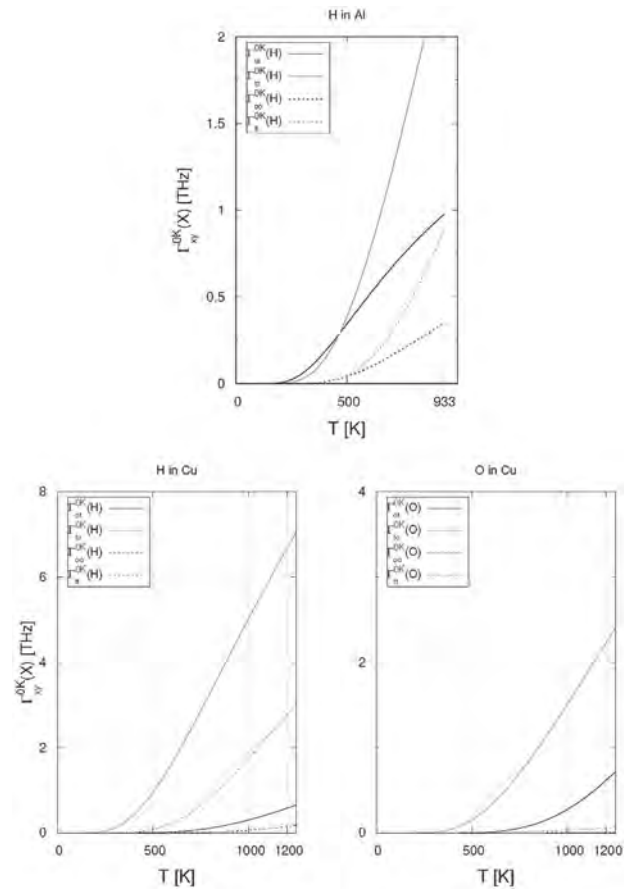

Fig. 2. Jump rates $\Gamma_{xy}(X)$ as a function of the temperature for different paths (ot and to direct jumps, oo and tt via M) for O and H atoms in Al and Cu. Jump rates were computed using values (energies and frequencies) at 0 K.

$$\Gamma = \frac{k_B T}{h} \frac{Z_{TS}}{Z_{EI}} e^{-\Delta E_m / k_B T} = \nu^* e^{-\Delta E_m / k_B T} \quad (1)$$

where ΔE_m corresponds to the (electronic) transition migration energy. Z_{TS} is the (vibrational) partition function for the transition state and Z_{EI} is the partition function for the initial position. Z is expressed by:

$$F = -k_B T \ln Z = k_B T \sum_{\mathbf{q}\nu} \ln\left(2 \sinh\left[-\frac{\hbar\omega_{\mathbf{q}\nu}}{2k_B T}\right]\right) \quad (2)$$

where $\omega_{\mathbf{q}\nu}$ are the frequencies of the ν mode in $\mathbf{q}$ point. Eq. (1) is valid regardless of the configuration of the transition state, i.e., whether only one imaginary mode is associated with the diffusing atom (first-order transition state) or several. The usual (high temperature approximation) formula of ν^* (see Wimmer et al. [2]) is as follows:

$$\nu^* = \frac{\prod_{i=1}^{3N-3} \omega^{EI}_{\mathbf{q}=\Gamma,i}}{\prod_{i=1}^{3N-4} \omega^{ET}_{\mathbf{q}=\Gamma,i}} \quad (3)$$

introduces the ratio between frequencies in the initial position and the ones in the transition state computed in the center of the Brillouin Zone ($\mathbf{q} = \Gamma$). However, when there are two (or three) imaginary frequencies, this usual formula does not apply, ν^* should be proportional to a frequency. We must thus employ the same formula but with partition functions given by eq. (2). These quantities can be examined even in cases where the transition state has many imaginaries frequencies, by eliminating the terms associated with these imaginary frequencies.

With these jump rates, we can now express explicit diffusion equations (D). In cases where paths of first-order transition states were considered only (here limited to direct *o*-*t* jumps), D is thus

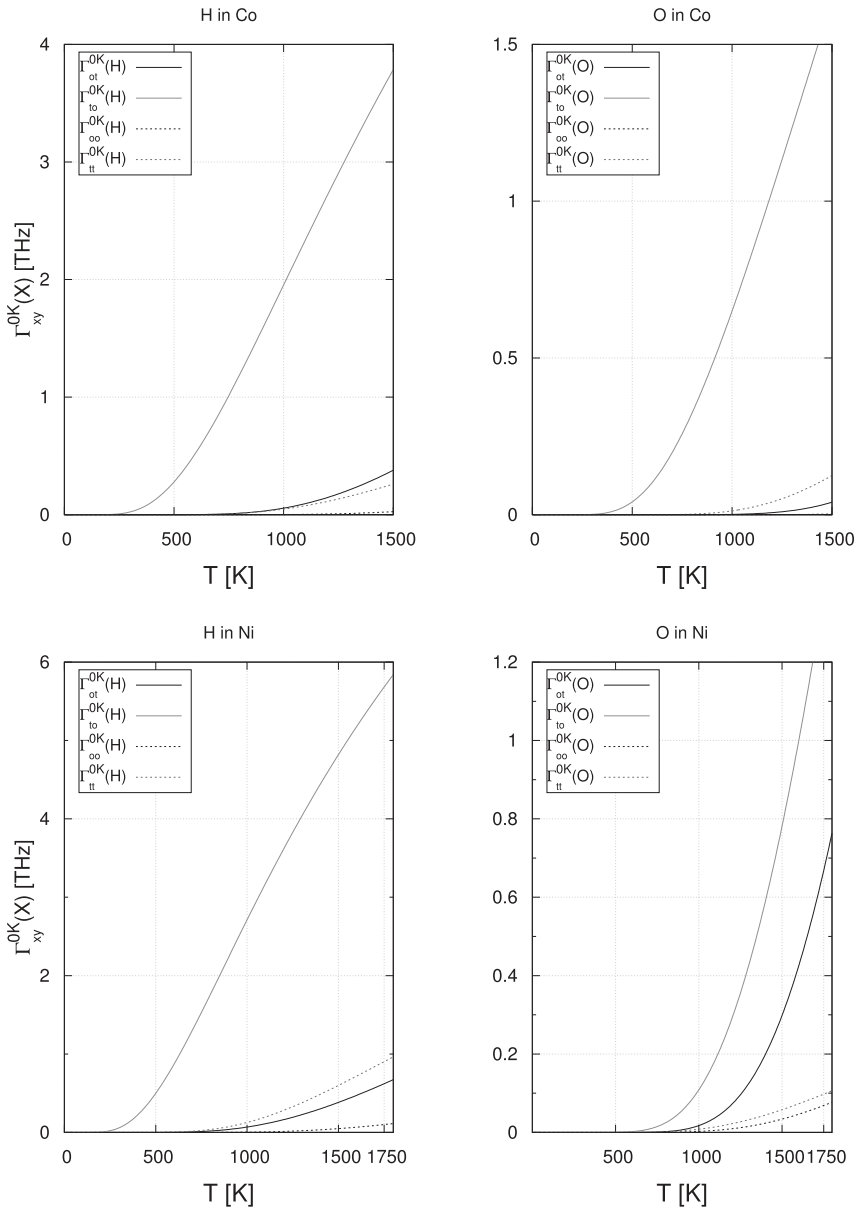

Fig. 3. Jump rates $\Gamma_{xy}(X)$ as a function of the temperature for different paths (*ot* and *to* direct jumps, *oo* and *tt* via *M*) for O and H atoms in Co and Ni. Jump rates were computed using values (energies and frequencies) at 0 K.

given by Refs. [2,4]:

$$D = \frac{a_o^2}{2} \frac{\Gamma_{to}\Gamma_{ot}}{\Gamma_{to} + 2\Gamma_{ot}} \tag{4}$$

where Γ_{to} (resp. Γ_{ot}) is the jump rate from the t (resp. o) to o (resp. t), and a_o the lattice parameter equal to 4.04, 3.61, 3.52, 3.52 and 3.95 Åfor Al, Cu, Co, Ni and Pd, respectively.

For higher-order transitions states, the diffusion coefficient is different. When leaving o (t) sites, atoms can either go directly to the t (o) sites as before, with a Γ_{ot} (Γ_{to}) probability, or go through the M sites, with a Γ_{oo} (Γ_{tt}) jump rate. Both direct and indirect paths to reach the nearest site led to the same type of displacement as before, however the probability was increased by the possibility to go through the M sites. When an interstitial crosses an M site (which is a 2TS) to reach either an o or a t site, we assumed that the atom can bifurcate and has the same probability of going towards the different sites (octahedral and tetrahedral). The diffusion coefficient (following the method of Landman et al. [12]) should thus be modified as follows (see details in Appendix):

$$\begin{aligned} D = \frac{a_o^2}{6}\Big[&16\,\Gamma_{oo}\Gamma_{tt}^2 + 12\,\Gamma_{ot}\Gamma_{tt}^2 + 20\Gamma_{oo}\Gamma_{tt}\Gamma_{to} + \\ &14\,\Gamma_{ot}\Gamma_{tt}\Gamma_{to} + 5\,\Gamma_{oo}\Gamma_{to}^2 + 3\,\Gamma_{ot}\Gamma_{to}^2\Big] / \\ &[(2\,\Gamma_{oo} + \Gamma_{tt} + 2\,\Gamma_{ot} + \Gamma_{to})(2\,\Gamma_{tt} + \Gamma_{to})] \end{aligned} \tag{5}$$

3. Results

To illustrate the impact of these new jumps, we will present results on different fcc-systems (Al, Co, Cu, Ni and Pd) and for two types of atoms (H and O). In Table 1, formation energies (E_f, in eV) and enthalpy energies, H_f, including the zero-point energy (ZPE) corresponding to the different sites (o, t and M) are summarized. The formation energy corresponds to:

$$E_f = E_o[n.M + X] - E_o[n.M] - \frac{1}{2}\mu[X_2] \tag{6}$$

where E_o are the DFT energy of fcc-systems with and without an impurity X. $\mu[X_2]$ corresponds to the chemical potential of the gas (H_2 or O_2). To compute migration energies, NEB calculations [13] were conducted with five intermediate images.

Results are in good agreement with the literature [2,4,5,15–18]. Some results show differences in formation energies. In the case of Cu, Korzhavyi et al. [15] kept fixed the shape of super-cells, that which necessarily induces larger energies (calculations were conducted at constant volume and not at constant pressure). Our results (difference in energy between t and o sites) on H and O in Co are in agreement with those of Liu et al. [5], and Korzhavyi [15] for Cu. Results on Al and Ni where extracted from previous results [4,14]. Moreover, some ZPEs differ slightly from what can be found in the literature. This is due to the approximation often used to compute the ZPEs. Here, we used the full expression computed on $20 \times 20 \times 20$ **q**-meshes (computed on $2 \times 2 \times 2$ super-cells). The reader should refer to the literature concerning the stability of sites: except H in Al and O in Pd, for which t sites are the more stable configurations, interstitials prefer to be located in o sites. Otherwise, regarding vibrational properties, we verified that (i) o and t are stable sites (all vibrations are real), (ii) atoms in M sites have two imaginary frequencies (i.e. unstable) and (iii) all direct transition states (o-t) have only one imaginary frequency (1TS). As explained above, due to its specific position, the M site is at the confluence of 4 configurations. As stated previously, we considered they were equivalent, this explains why M sites have two imaginary frequencies associated only with the interstitial element.

Regarding migration energies, differences with the literature were noticed, specially in the case of H and O in Cu [15]. As explained above, Korzhavyi et al. [15] did not relax shapes of supercells in their simulations (for o, t sites and transition states as well), we can therefore assume that they strongly overestimated activation energies, specially in the case of oxygen, where distortions are most important They found about 0.6 eV between o and t sites for O atoms, whereas we found 0.36 eV. In contrast, some of our results are similar to those found in the literature for others systems. For instance, Liu et al. [5], in their study of H and O diffusion in Co (GGA values), found activation energies (0.47/0.17 eV for H and 1.03/0.28 eV for O) in excellent agreement with ours (0.46/0.17 for H and 0.94/0.24 eV for O, see Table 1). For other

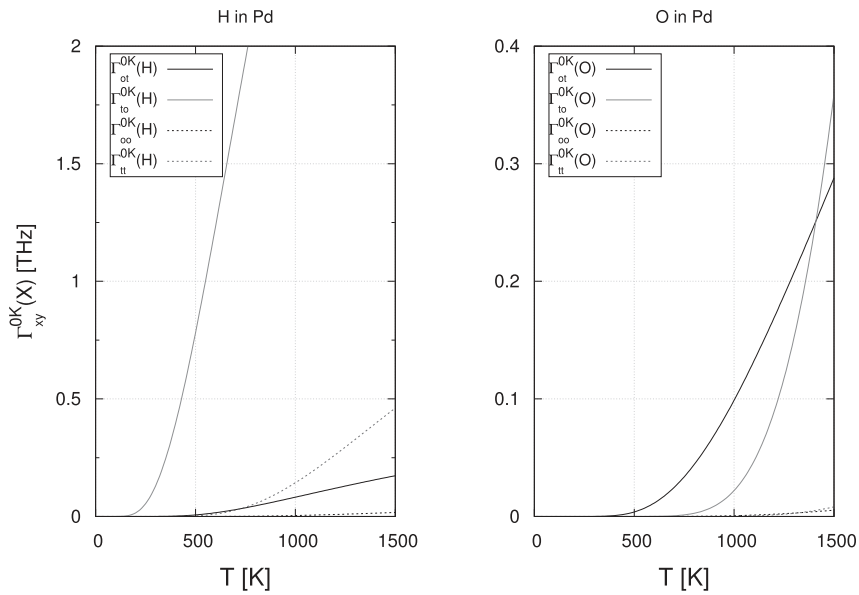

Fig. 4. Jump rates $\Gamma_{xy}(X)$ as a function of the temperature for different paths (ot and to direct jumps, oo and tt via M) for O and H atoms in Pd. Jump rates were computed using values (energies and frequencies) at 0 K.

systems (Al and Ni specifically [1,19]), our results are in good agreement with the literature.

For all jumps, atomic jump rates ($\Gamma_{xy}(X)$) were calculated using vibrational Helmholtz energies which were in turn computed using IFCs. xy represents the jump from x to y configurations. Their evolutions according to the temperature were displayed on Figs. 2–4.

Contrary to what expected, we note that, in some cases (H in Ni and Pd, O in Co and Pd), the jump rate associated to the 2TS (specially Γ_{tt}) is not negligible compared to the jump rates of 1TS. In other cases (H in Al and Cu), Γ_{to} is even lower than Γ_{tt}. The probability to jump through the M site increases the total jump probability and increases D, especially as soon as we approach melting temperatures. This can be partially explained by the small value of migration energies.

The diffusion coefficients were then computed using both equations (4) and (5) for comparison. Diffusivities as a function of temperature are depicted on Figs. 5 and 6. When experimental measurements are available, we added them on figures.

We can now compare our theoretical results with experimental data when they exist. First, for H in Ni, Cu and Pd, theory and experiments are in good agreement: slopes, associated with the

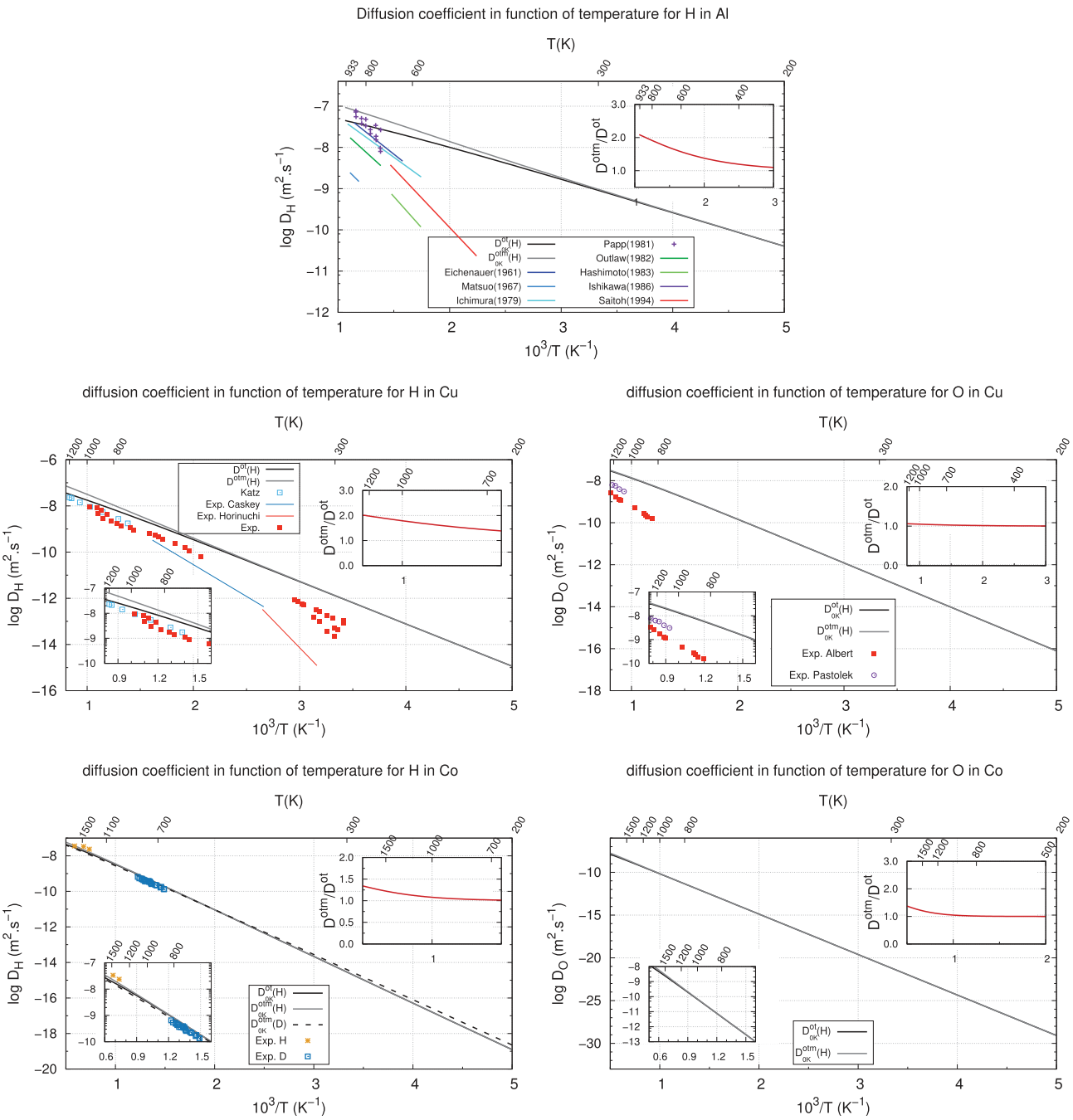

Fig. 5. Diffusion coefficients (in m^2s^{-1}) as a function of T and 10^3/T taking into account either only o-t direct path or passage through M sites. We also give the ratio between both equations (in red). Experimental data were extracted from literature: H in Al from Ref. [20], H in Cu [21–24], O in Cu [25,26]. (For interpretation of the references to colour in this figure legend, the reader is referred to the Web version of this article.)

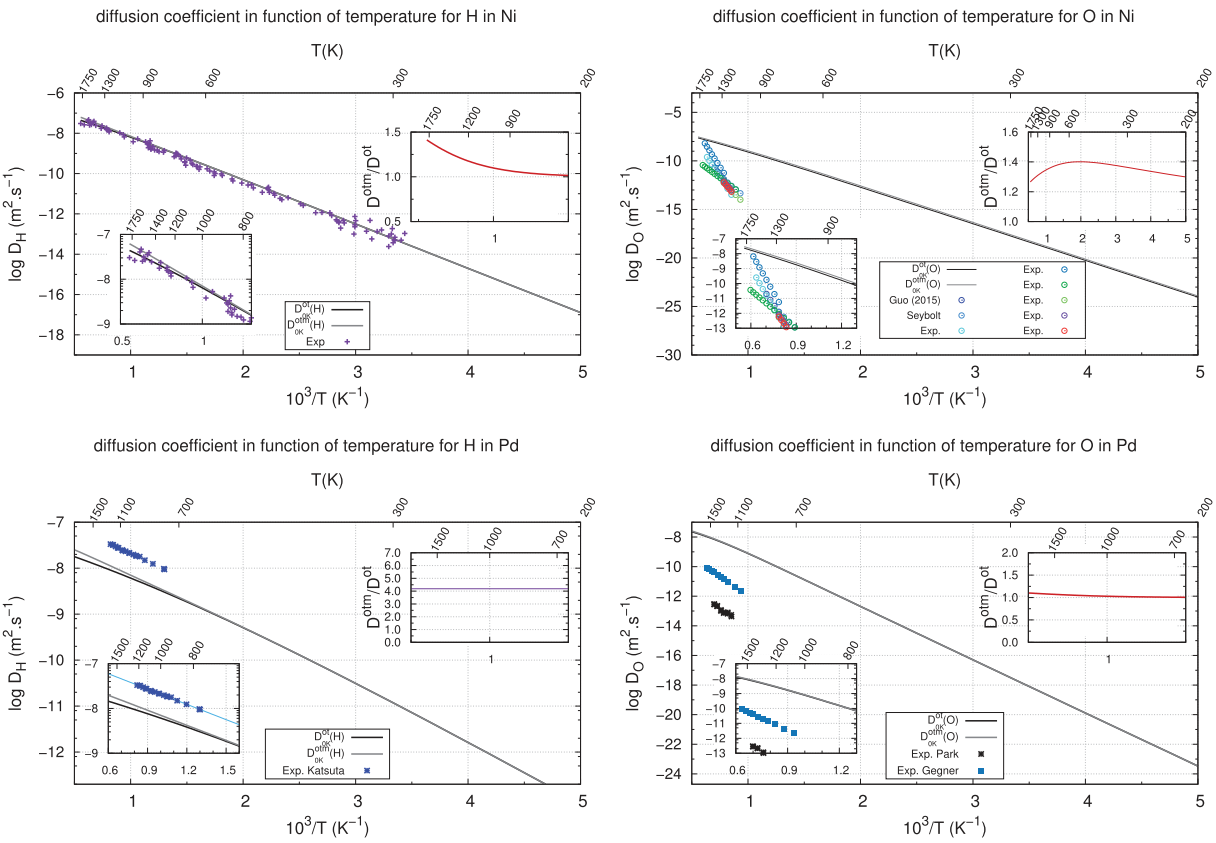

Fig. 6. Diffusion coefficients (in m^2s^{-1}) as a function of T and 10^3/T taking into account either only *o-t* direct path or passage through *M* sites. We also give the ratio between both equations (in red). Experimental data were extracted from literature: H in Pd [27], O in Pd [28,29], H in Ni extracted from Wimmer et al. [2] and O in Ni from Ref. [30]. (For interpretation of the references to colour in this figure legend, the reader is referred to the Web version of this article.)

activation energy, E_a, and prefactors (D_o) are in excellent agreement, see Table 2. At high T, higher-order transition states allow faster diffusion of H atoms and therefore increase *D*. In the case of Pd, our values of *D* are slightly smaller than experimental ones. This difference may be due to an underestimation of frequencies. In the case of H atoms in Cu, Nazarov's [31] and Wang's works [19] could explain the small overestimation of *D* at low T. Nazarov showed that hydrogen-vacancy interactions in copper are strong. From Wang's analysis, we can assume that clusters are expected to modify vacancy concentration thereby changing hydrogen diffusivity at low T. Near the melting point however, where trapping is not thermodynamically favored, all these effects thus become negligible (see earlier works [19,32]), and our data match Katz's values [22].

In the case of H atoms in Al, one notes that the calculated diffusivity is in good agreement with the literature values only at high T (see results summarized by Young et al. [20]). When the temperature decreases, the slopes become significantly different. This strong discrepancy could be explained by the fact that H can form easily VH_n clusters [33,34]. It is therefore not the diffusion of the isolated H atom in the network that should be considered, but rather a more complex diffusion mechanism taking into account the migration of VH_n clusters.

In the case of oxygen, we note that, for all metals with existing experimental data (Cu, Ni and Pd), there is an important discrepancy with theoretical values. Theoretical values are always higher than experimental data. For O diffusivity in Cu, Ni and Pd, one notes a strong similarity, the observed diffusion is much slower than expected. O atoms diffuse theoretically faster than expected. It

Table 2
Activation energy (E_a, in eV) and prefactor (D_o, in $10^{-6}m^2/s$) of the diffusion coefficients, fitted from theoretical and experimental data. We compare the fitted values (between [300; 1200] K) obtained taking into account or not the 2TS (noted without/with 2TS).

		E_a		D_o	
		Theo.	Exp.	Theo.	Exp.
H	Al	0.138/0.175	–	0.25/0.82	–
H	Cu	0.318/0.366	0.435 [21]	0.7/2.2	1.7 [21]
O	Cu	0.357/0.361	0.617 [26]	0.8/0.9	7.8
H	Co	0.479/0.501	0.482 [22]	0.8/1.2	0.6 [22]
O	Co	0.933/0.968	–	3.2/5.1	–
H	Ni	0.407/0.424	0.410 [22]	0.7/0.9	0.7 [22]
O	Ni	0.75/0.667	1.5–2.3 [30]	2.1/2.4	–
H	Pd	0.208/0.224	0.226 [27]	0.07/0.09	0.28 [27]
O	Pd	0.692/0.697	1.06–1.02 [28,29]	2.4/2.6	2.2 [28]

Table 3
Vacancy (H^f_{1v}, in eV) and segregation energies of H and O atoms in a vacancy (E_{seg}, in eV). We also report VX-cluster formation energies (H^f_{vx}, in eV) in Al, Cu, Ni, Co and Pd. *o* and *t* sites inside the vacancy were considered, see details in Connétable et al. [18]. Some data were extracted from the literature.

		X	H^f_{1v}	H^f_{vx}	E_{seg}
Al	[34]	H	0.632	1.017	-0.335^t
Ni	[19]	H	1.427	1.154	-0.273°
	[18]	O	1.427	$0.745^\circ/0.745^t$	$-1.14^\circ/-1.14^t$
Co		O	1.830	$0.755^\circ/0.991^t$	$-0.99^\circ/-0.71^t$
Cu	[31]	H	1.099	0.84	-0.26°
		O	1.099	$0.439^\circ/0.523^t$	$-0.75^\circ/-0.66^t$
Pd	[31]	H	1.165	0.96	-0.20^t
		O	1.165	$1.292^\circ/1.072^t$	$-0.53^\circ/-0.74^t$

should be noted, that experimentally it is not the diffusion coefficient that is directly measured but the product solubility-diffusivity of oxygen in solid as a function of temperature. We note there is a great discrepancy among experimental values which depends on the experimental approach and the oxygen concentration (either measured or approximated values from earlier experimental fits) used for the calculation of diffusion coefficients, as showed by Prillieux [30] in the case of Ni. Again, this discrepancy can be explained by the formation of clusters. In the case of O in Ni [18], it has been clearly shown that there is a strong interaction between metal and O atoms, promoting the formation of clusters which, after a thermodynamic analysis, are present in large quantities even at high temperatures. O atoms do not diffuse alone in metallic systems. By studying oxygen diffusivity in Ni using molecular dynamics simulations, Fang [35] also explains discrepancies between theory and experience with the trapping of O atoms by vacancies, but without formalizing the effect. By studying H trapping by vacancies in Ni, Wang [19] demonstrated that (i) Oriani's model [36] adequately captures the physics in the case of trapping, and (ii) the effect is limited to high vacancy concentrations at low T (in which case, the hydrogen segregation energy is low and the vacancy formation energy is high). At high temperature, VH_n clusters are broken [32].

We thus applied the Oriani model to try to correct our diffusion coefficients, by introducing the possibility of trapping by vacancies.

In its model, Oriani introduces two quantities: the number of traps n_t which can be approximated by using the number of sites n_s in the vacancy ($n_s = 6$ or 8 for *o* or *t* sites, respectively) multiplied by the vacancy concentration, $\exp(-H^f_{1v}/k_BT)$, and the probability of segregation of an X atom in the vacancy, $\exp(-E_{seg}/k_BT)$. The effective diffusion of interstitial solutes in the presence of traps is thus given by:

$$D_{eff} \simeq \frac{D}{1 + n_s \exp\left[-\left(H^f_{1v} + E_{seg}\right)/k_BT\right]} \tag{7}$$

Parameters are summarized in Table 3. We found that, in all cases, the correction is negligible, $D_{eff}/D \simeq 1$, even in the case of O atoms, where the oxygen-vacancy interaction is strong (ranging from −1.1 to −0.7 eV). With eq. (7), the amount of traps, given by the thermal vacancy concentration, is not enough to reduce significantly the diffusion coefficients. More complex models (including more traps) must therefore be used to analyze oxygen transport in metals in order to reproduce experimental data, see the work of Schuler et al. [37].

We can now discuss the influence of 2TS on diffusion coefficient. We note that, at low T, the main contribution in the diffusivity value corresponds to the direct path. As a consequence, when ignoring *M* sites we do not change atomistic mechanisms, the corresponding paths have negligible impact on coefficient of diffusion. In some cases, however, *D* increases at higher temperatures, especially for H atoms, even if the increase is limited to a maximum factor 2 in our results. To jump from *o* sites through *M*, the energy is always high, Γ_{oo} is thus relatively low, but since the jump rates Γ_{tt} are not negligible at high T, these jumps (*t*-*t*) could occur.

4. Conclusion

We showed that at low temperature the atomistic process is clearly controlled by direct jumps, this was an expected result. The jump rates Γ_{ot} and Γ_{to} are thus significantly higher than jump rates of second-order transition states. By including higher-order transition states, the diffusion of species can be increased two-fold in some cases. The effect of second-order transition states on the diffusion coefficient is thus limited in our case. If high-order transition states can be ignored in first-approximation for fcc-systems as shown here, they must be examined for other systems, as bcc systems for instance. Similarly, in the case where several equivalent sites are present locally (segregation in vacancies, in grain boundaries or dislocations), higher-order transition states should be taken into account.

The present work also shows that, in the case of O atoms, theory always overestimates diffusivity in metallic systems, probably due to more complex diffusion mechanisms that include vacancy-oxygen clusters, and to the fact that for hydrogen, experimental results above ambient temperature can be reproduced with a high accuracy. The Oriani model is not adequate to correct theoretical results in first-approximation.

Acknowledgments

This work was performed using HPC resources from CALMIP (Grant 2018-p0749) and GENCI-CINES (Grant A0020907722). Authors acknowledge Pr. C. Raynaud (Institute Charles Gerhardt of Montpellier) and D. Tanguy (ILM Lyon) for their comments and advices.

Multi-states model

In the case where there are two stable sites (*t* and *o*) and several possible jumps, i.e. the direct *t*-*o* jump and those passing through *M* sites, *D* is expressed by (following the Landman's method [12]):

$$D = \frac{a_o^2}{6}\Big[16\,\Gamma_{oMo}\Gamma^2_{tMt} + 12\,\Gamma_{ot}\Gamma^2_{tMt} + 20\,\Gamma_{oo}\Gamma_{tMt}\Gamma_{to} + 14\,\Gamma_{ot}\Gamma_{tMt}\Gamma_{to} + 5\,\Gamma_{oMo}\Gamma^2_{to} + 3\,\Gamma_{ot}\Gamma^2_{to}\Big] / \left[(2\,\Gamma_{oMo} + \Gamma_{tMt} + 2\,\Gamma_{ot} + \Gamma_{to})(2\,\Gamma_{tMt} + \Gamma_{to})\right] \tag{8}$$

We must first identify the number of non-equivalent positions in the primitive cell. In the fcc system, there are two non-equivalent *t* sites (labeled t_1 and t_2) and one *o* site. Then, we must identify

different possible jumps to leave each sites. Two quantities are thus required: the Laplace transform of the waiting time density matrix, $\underline{\psi}(u)$, and the Fourier transform matrix of the displacements of X in Ni, $\underline{p}(k)$.

$\underline{\psi}(u)$ is given by:

$$\underline{\psi}(u) = \begin{array}{c} \\ o \\ t_1 \\ t_2 \end{array}\begin{array}{c} \begin{array}{ccc} o & t_1 & t_2 \end{array} \\ \begin{bmatrix} \frac{12\Gamma'_{oM}}{K_o} & \frac{4\Gamma_{to}+12\Gamma'_{tM}}{K_t} & \frac{4\Gamma_{to}+12\Gamma'_{tM}}{K_t} \\ \frac{12\Gamma'_{oM}+4\Gamma_{ot}}{K_o} & 0 & \frac{6\Gamma'_{tM}}{K_t} \\ \frac{12\Gamma'_{oM}+4\Gamma_{ot}}{K_o} & \frac{6\Gamma'_{tM}}{K_t} & 0 \end{bmatrix} \end{array} \tag{9}$$

where $K_o = 36\Gamma'_{oM} + 8\Gamma_{ot} + u$ and $K_t = 18\Gamma'_{tM} + 4\Gamma_{to} + u$. Γ_{xy} is the probability of escape from internal state x to state y.

For instance, when X is in o (resp. t), it can leave o (resp. t) and jump directly in $t_{1,2}$ (resp. o), with the probability Γ_{ot} (resp. Γ_{to}) or jump in the 2TS M, with the probability Γ'_{oM} (resp. Γ'_{tM}). In M, X can fall, with the same probability, either in $t_{1,2}$ (two possibilities) or in o (one), thus $\Gamma'_{om} = \Gamma_{om}/3$. With the same argument, we suppose $\Gamma'_{tM} = \Gamma_{tMt}/3$ It is not possible to jump directly between two different equivalent t sites.

$\underline{p}(k)$ is given by:

$$\underline{p}(k) = \begin{array}{c} \\ o_1 \\ t_1 \\ t_2 \end{array}\begin{array}{c} \begin{array}{ccc} o_1 & t_1 & t_2 \end{array} \\ \begin{bmatrix} A_{oMo} & A_{t_1o} & A_{t_2o} \\ A_{ot_1} & 0 & A_{t_2Mt_1} \\ A_{ot_2} & A_{t_1Mt_2} & 0 \end{bmatrix} \end{array} \tag{10}$$

where

$$\begin{aligned} A_{oM_o} &= \Big[e^{i\,l\,k_1} + e^{-i\,l\,k_1} + e^{i\,l\,k_2} + e^{-i\,l\,k_2} + e^{i\,l\,k_3} + \\ &\quad e^{-i\,l\,k_3} + e^{i\,l\,(k_1-k_2)} + e^{-i\,l\,(k_1-k_2)} + e^{i\,l\,(k_3-k_2)} + \\ &\quad e^{-i\,l\,(k_3-k_2)} + e^{i\,l\,(k_1-k_3)} + e^{-i\,l\,(k_1-k_3)}\Big]/12 \\ A_{t_1Mt_2} &= \Big[e^{i\,l\,k_1} + e^{i\,l\,k_2} + e^{i\,l\,k_3} + \\ &\quad e^{i\,l\,(k_1+k_2)} + e^{i\,l\,(k_2+k_3)} + e^{i\,l\,(k_1+k_3)}\Big]/6 \\ A_{t_2Mt_1} &= \Big[e^{-i\,l\,k_1} + e^{-i\,l\,k_2} + e^{-i\,l\,k_3} + \\ &\quad e^{-i\,l\,(k_1+k_2)} + e^{-i\,l\,(k_2+k_3)} + e^{-i\,l\,(k_1+k_3)}\Big]/6 \\ A_{t_1o} &= \Big[1 + e^{-i\,l\,k_1} + e^{-i\,l\,k_2} + e^{-i\,l\,k_3}\Big]/4 \\ A_{ot_1} &= \Big[1 + e^{i\,l\,k_1} + e^{i\,l\,k_2} + e^{i\,l\,k_3}\Big]/4 \\ A_{t_2o} &= \Big[1 + e^{i\,l\,k_1} + e^{i\,l\,k_2} + e^{i\,l\,k_3}\Big]/4 \\ A_{ot_2} &= \Big[1 + e^{-i\,l\,k_1} + e^{-i\,l\,k_2} + e^{-i\,l\,k_3}\Big]/4 \end{aligned} \tag{11}$$

with $l = a_o\sqrt{2}/2$. In $\underline{p}(k)$, we only consider the final displacement, this is why $A_{t_{1,2}o}$ and $A_{o,t_{1,2}}$ have the same expressions when the jump goes through M or not.

To derive D, we then followed the same approach than Wu et al. [38].

References

[1] C. Wolverton, V. Ozolins, M. Asta, Phys. Rev. B 69 (2004), 144109.
[2] E. Wimmer, W. Wolf, J. Sticht, P. Saxe, C. Geller, R. Najafabadi, G. Young, Phys. Rev. B 77 (2008), 134305.
[3] Y. Wang, D. Connétable, D. Tanguy, Phys. Rev. B 91 (2015), 094106.
[4] M. David, D. Connétable, J. Phys. Condens. Matter 29 (2017), 455703. http://stacks.iop.org/0953-8984/29/i=45/a=455703.
[5] W. Liu, N. Miao, L. Zhu, J. Zhou, Z. Sun, Phys. Chem. Chem. Phys. 19 (2017) 32404. https://doi.org/10.1039/C7CP07208B.
[6] G. Kresse, J. Hafner, Phys. Rev. B 47 (1993) 558.
[7] G. Kresse, D. Joubert, Phys. Rev. B 59 (1999) 1758.
[8] J. Perdew, K. Burke, M. Ernzerhof, Phys. Rev. Lett. 78 (1997) 1396.
[9] H. Monkhorst, J. Pack, Phys. Rev. B 13 (1976) 5188.
[10] A. Togo, F. Oba, I. Tanaka, Phys. Rev. B 78 (2008), 134106.
[11] H. Eyring, J. Chem. Phys. 3 (1935) 107.
[12] U. Landman, M.F. Shlesinger, Phys. Rev. B 19 (1979) 6207. http://link.aps.org/doi/10.1103/PhysRevB.19.6207.
[13] G. Henkelman, B. Uberuaga, H. Jónsson, J. Chem. Phys. 113 (2000) 9901.
[14] M. David and D. Connétable (2018), submitted.
[15] P. Korzhavyi, R. Sandström, Comput. Mater. Sci. 84 (2014) 122. ISSN 0927-0256, http://www.sciencedirect.com/science/article/pii/S0927025613007489.
[16] R. Nazarov, T. Hickel, J. Neugebauer, Phys. Rev. B 85 (2012), 144118.
[17] B. Amin-Ahmadi, D. Connétable, M. Fivel, D. Tanguy, R. Delmelle, S. Turner, L. Malet, S. Godet, T. Pardoen, J. Proost, et al., Acta Mater. 111 (2016) 253. ISSN 1359-6454, http://www.sciencedirect.com/science/article/pii/S1359645416302166.
[18] D. Connétable, M. David, A. Prillieux, D. Young, D. Monceau, J. Alloys Compd. 708 (2017) 1063. https://doi.org/10.1016/j.jallcom.2017.03.018.
[19] Y. Wang, D. Connétable, D. Tanguy, Acta Mater. 103 (2016) 334.
[20] G. Young, J. Scully, Acta Mater. 46 (1998) 6337. ISSN 1359-6454, http://www.sciencedirect.com/science/article/pii/S1359645498003334.
[21] H. Magnusson, K. Frisk, J. Phase Equil. Diffusion 38 (2017) 65. ISSN 1863-7345, https://doi.org/10.1007/s11669-017-0518-y.
[22] L. Katz, M. Guinan, R.J. Borg, Phys. Rev. B 4 (1971) 330. https://link.aps.org/doi/10.1103/PhysRevB.4.330.
[23] H. Horinouchi, M. Shinohara, T. Otsuka, K. Hashizume, T. Tanabe, J. Alloys Compd. 580 (2013) S73. ISSN 0925-8388, sI : MH2012, http://www.sciencedirect.com/science/article/pii/S0925838813008761.
[24] H.-B. Zhou, Y. Zhang, X. Ou, Comput. Mater. Sci. 79 (2013) 923. ISSN 0927-0256, http://www.sciencedirect.com/science/article/pii/S0927025613004539.
[25] J. Orszagh, F. Bouillon, Mem. Sci. Rev. Met. 70 (1973) 319.
[26] E. Albert, R. Kirchheim, H. Dietz, Scr. Metall. 15 (1981) 673.
[27] H. Katsuta, R. Farraro, R. McLellan, Acta Metall. 27 (1979) 1111. ISSN 0001-6160, http://www.sciencedirect.com/science/article/pii/0001616079901287.
[28] J. Gegner, G. Hörz, R. Kirchheim, J. Mater. Sci. 44 (2009) 2198. ISSN 1573-4803, https://doi.org/10.1007/s10853-008-2923-4.
[29] J.-W. Park, C.J. Altstetter, Scr. Metall. 19 (1985) 1481. ISSN 0036-9748, http://www.sciencedirect.com/science/article/pii/0036974885901553.
[30] A. Prillieux, Hydrogen and Water Vapour Effects on Oxygen Solubility and Diffusivity in High Temperature Fe-ni Alloys, 2017. http://oatao.univ-toulouse.fr/18676/.
[31] R. Nazarov, T. Hickel, J. Neugebauer, Phys. Rev. B 89 (2014), 144108. http://link.aps.org/doi/10.1103/PhysRevB.89.144108.
[32] D. Tanguy, Y. Wang, D. Connétable, Acta Mater. 78 (2014) 135.
[33] D. Tanguy, Corrosion 72 (2016) 297. https://doi.org/10.5006/1854.
[34] D. Connétable, M. David, J. Alloys Compd. 748 (2018) 12. ISSN 0925-8388, http://www.sciencedirect.com/science/article/pii/S0925838818309423.
[35] H. Fang, S. Shang, Y. Wang, Z. Liu, D. Alfonso, D. Alman, Y. Shin, C. Zou, A. van Duin, Y. Lei, et al., J. Appl. Phys. 115 (2014), 043501.
[36] R. Oriani, Acta Metall. 18 (1970) 147.
[37] T. Schuler, M. Nastar, Phys. Rev. B 93 (2016), 224101. https://link.aps.org/doi/10.1103/PhysRevB.93.224101.
[38] H.H. Wu, D.R. Trinkle, Phys. Rev. Lett. 107 (2011), 045504. http://link.aps.org/doi/10.1103/PhysRevLett.107.045504.